Journal of Visualization, Vol. 1, No. 2 (1998) 161-170

Statistical Approach to the Measurement of Velocity Field

Nishio, S.* and Okuno, T.*

* Department of Marine System Engineering, Osaka Prefecture University, Sakai, Osaka, 599-8531 Japan.

Received 17 March 1998.
Revised 16 July 1998.

***Abstract*:** Present paper describes the principle and applications of a velocity measurement using statistical analysis of visualized flow images. The authors have developed a new algorithm for the measurement using the passing probability of a particle. It is known that this kind methods gives the total flow speed at each pixel unit. In this study, the method is extended by forming the governing equation using the Lagrange's differentiation. The process is similar to the so-called spatio-temporal derivative method. The extension of the equation enables to measure the velocity components with the help of the statistical technique. The idea is based on the fact that the temporal derivative of luminance function is proportional to the vector product of the flow velocity and the gradient of luminance function in space which gives the velocity component normal to the edge of particle image. This is easy to apply on the three-dimensional flow field.

***Keywords*:** PIV, statistical analysis, spatio-temporal derivative, flow velocity measurement, wake measurement.

1. Introduction

Flow visualization has been a useful technique to catch up the physical phenomena in flow field. Recent developments of the digital image processing produce new measurement techniques which quantify the flow information in images such as flow velocity. A number of papers on the development of the technique have been published already. The measurement technique enables to obtain the instantaneous velocity field realize the non-intrusive measurement and reduce the consuming time for measurement drastically.

For steady flows, the time-averaged velocity distribution in addition of the instantaneous velocity is also useful in the practical sense. The so-called spatio filtering method (Kobayashi, 1980; Katoh, 1992) is a most popular one for the measurement of time-mean speed of a moving obstacle. It is, however, difficult to determine the suitable optical filter, which depends on the flow field. The authors have developed a measurement technique having high spatio resolution (Okuno et al., 1993; Okuno et al., 1994). The measurement technique obtains the time-averaged velocity speed directly from the image data, i.e., the technique does not need to identify the velocity vectors in each image. The technique gives flow speed at every pixel unit. Nishio et al. (1995, 1996) introduced the statistical approach into the analysis of the measurement . The flow speed can be derived with the method, and it is still useful from the practical point of view. In this paper, the statistical process is extended to the measurement of the velocity vectors by considering the governing equation using the Lanrange's differentiation and introducing the stream line coordinate system.

2. Probability of Particle Passing

Present measurement technique is based on the fact that the passing probability of a particle is proportional to the local flow speed. In this paper, as Figure 1 shows the schematic view of the particle in the flow field, the particle

positions are represented by (x, y, z) using a Cartesian co-ordinate system, and the sheet illumination is normal to the x-axis. The stream line co-ordinate system (ξ, η, ζ) is also used where ξ shows the local flow direction, and the measurement point is represented by $\xi = \xi_0$. The luminance at $\xi = \xi_0$ looks like heart beat signal, and the beat speed is proportional to the absolute value of flow speed if the particle concentration is constant and uniform through the measurement.

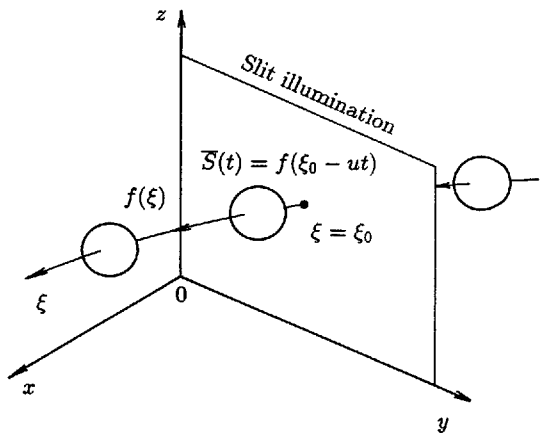

Fig. 1. Schematic view of a particle passing through a sheet illumination and coordinate systems in the flow field.

Non-uniformity of the particle concentration in space would be found from the experimental condition. In this case, the flow speed is given by the ratio of the possibility of particle passing and the particle concentration. Considering a tracer particle which passes through the sheet illumination at $\xi = \xi_0$, the measured luminance function is given as $\overline{S}(t)$. f shows the luminance function along the stream lines when illumination of the same, is given over the whole flow field. Then $\overline{S}(t)$ is shown with function f as follows.

$$\overline{S}(t) = f(\xi_0 - ut), \tag{1}$$

where u shows the velocity at $\xi = \xi_0$.

The luminance function f also can be regarded as the function of position (x, y, z) and time t. When the fluid at a point $P(x - \Delta x, y - \Delta y, z - \Delta z)$ moves to $P'(x + \Delta x, y + \Delta y, z + \Delta z)$, the difference of luminance between these two points can be expressed as shown in Eq.(2).

$$f(x+\Delta x, y+\Delta y, z+\Delta z, t+\Delta t) - f(x-\Delta x, y-\Delta y, z-\Delta z, t-\Delta t) = g(x, y, z, t, \Delta t), \tag{2}$$

where $g(x, y, z, t, \Delta t)$ shows the gradient of back ground illumination which is a function of position, time and time interval. When the change of the luminance function and the velocity field are smooth enough, those values can be expressed using the Taylor's expansion around the point (x, y, z, t).

$$f(x+\Delta x, y+\Delta y, z+\Delta z, t+\Delta t) = f(x, y, z, t) + \frac{\partial f}{\partial x}\Delta x + \frac{\partial f}{\partial y}\Delta y + \frac{\partial f}{\partial z}\Delta z + \frac{\partial f}{\partial t}\Delta t + O(\delta^2), \tag{3}$$

$$\Delta x = u\Delta t + \frac{1}{2}\left\{u\frac{\partial u}{\partial x} + v\frac{\partial u}{\partial y} + w\frac{\partial u}{\partial z}\right\}(\Delta t)^2 + O(\delta^3). \tag{4}$$

Δy, Δz can be expanded as same as Δx. By substituting them into Eq.(2) with assuming that the higher order terms are small enough, the following equation which shows the governing equation of the gradient method, is obtained (Fukinuke, 1981; Horn et al., 1981; Hildreth, 1984; Ando, 1989; Okuno et al., 1991).

$$\frac{\partial f}{\partial t} + u\frac{\partial f}{\partial x} + v\frac{\partial f}{\partial y} + w\frac{\partial f}{\partial z} = \lim_{\Delta t \to 0}\frac{g(x, y, z, t, \Delta t)}{2\Delta t} \tag{5}$$

The flow velocity is expressed by (u_ξ, u_η, u_ζ) when the stream line co-ordinate system is introduced, and $u_\eta = u_\zeta = 0$ because ξ shows the local velocity direction. Therefore the governing equation is expressed as follows.

$$\frac{\partial f}{\partial t} + u_\xi \frac{\partial f}{\partial \xi} = \lim_{\Delta t \to 0} \frac{g(\xi, \eta, \zeta, t, \Delta t)}{2\Delta t} \tag{6}$$

When the gradient of back ground illumination, $g(\xi, \eta, \zeta, t, \Delta t)$, is negligibly smaller than the change of luminance in time Δt, the time averaged flow speed $|\bar{u}_\xi|$ is obtained by applying the time mean operation as shown in Eq.(7).

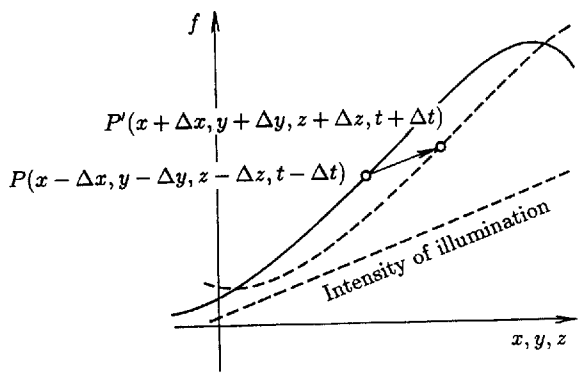

Fig. 2. Principle of the spatio-temporal derivative method.

$$|\bar{u}_\xi| = \frac{\frac{1}{T}\int_0^T \left|\frac{\partial f}{\partial t}\right| dt}{\frac{1}{T}\int_0^T \left|\frac{\partial f}{\partial \xi}\right| dt} \tag{7}$$

Equation (7) shows that the time averaged flow speed is given by the ratio of the statistical values of the derivatives of luminance in time and space. Furthermore, Equation (7) can be expressed with the statistical values, since the luminance function is assumed here to be a stationary random process and the expectations are equal to the corresponding temporal averages.

$$|\bar{u}_\xi| = \frac{E\left[\left|\frac{\partial f}{\partial t}\right|\right]}{E\left[\left|\frac{\partial f}{\partial \xi}\right|\right]} \tag{8}$$

where the operator $E[\ ]$ shows the ensemble average. Equation (8) shows that the present analysis does not need the successive images in time, but the random sampled. Usually the spatio derivatives of luminance along the stream line, $\partial f/\partial \xi$, cannot be known without flow field data. However, since it is possible to assume the isotropic local particle concentration, the following relationship can be used.

$$E\left[\left|\frac{\partial f}{\partial \xi}\right|\right] = E\left[\left|\frac{\partial f}{\partial x}\right|\right] = E\left[\left|\frac{\partial f}{\partial y}\right|\right] = E\left[\left|\frac{\partial f}{\partial z}\right|\right] \tag{9}$$

Equation (9) shows that $\partial f/\partial \xi$, can be estimated from the spatio derivative of the flow image visualized on sheet illumination both in the case of two- and three-dimensional case.

3. Measurement of Velocity Vectors

Equation (5) shows the governing equation of the spatio-temporal derivative method, and also the general form of the change of luminance in visualized flow images. In the previous section, the flow speed is obtained by introducing the stream line co-ordinate system. However, the velocity components cannot be obtained with them. In this section, the principle of the measurement of velocity vectors using statistical approach is described.

When the gradient of the background luminance is negligibly smaller than the change of luminance, the governing equation can be expressed as follows.

$$\frac{\partial f}{\partial t}+u\frac{\partial f}{\partial x}+v\frac{\partial f}{\partial y}+w\frac{\partial f}{\partial z}=0. \tag{10}$$

Assuming the local uniformity of velocity field, and applying the least square technique, the velocity vectors have been obtained by the spatio-temporal derivative method. Equation (10) can be regarded as the summation of the temporal derivative term and the inner-product between the velocity vector $\boldsymbol{u}(u, v, w)$ and the gradient of luminance function ∇f. Then Equation (10) can be re-written into the following vector notation as shown in Eq.(11), and the normalized form in Eq.(12).

$$\boldsymbol{u}\cdot\nabla f+\frac{\partial f}{\partial t}=0, \tag{11}$$

$$\alpha_x u+\alpha_y v+\alpha_z w+\beta=0, \tag{12}$$

where $\alpha_x=(\partial f/\partial x)/h$, $\alpha_y=(\partial f/\partial y)/h$, $\alpha_z=(\partial f/\partial z)/h$, $\beta=(\partial f/\partial t)/h$, $h=\{(\partial f/\partial x)^2+(\partial f/\partial y)^2+(\partial f/\partial z)^2\}^{1/2}$, and also, $\alpha_x^2+\alpha_y^2+\alpha_z^2=1$. The unit vector $\boldsymbol{n}=(\alpha_x, \alpha_y, \alpha_z)$ shows the direction of maximum gradient of the luminance function, and Eq.(12) can be expressed as,

$$\boldsymbol{n}\cdot\boldsymbol{u}+\beta=0. \tag{13}$$

When binarization is applied on the images, $\boldsymbol{n}$ represents the normal vector of the particle image boundary as shown in Fig. 3. Then Eq.(13) shows that the temporal derivative of luminance function, β, gives the velocity component normal to the edge of particle image. The appearance rate of normal vector $\boldsymbol{n}$ is constant in any direction because the particle images are usually round and no deflection to any particular direction. Therefore, it is possible to obtain the velocity direction through statistical analysis of the distribution of $-\beta\boldsymbol{n}=(-\beta\alpha_x, -\beta\alpha_y, -\beta\alpha_z)$. For the two-dimensional flow field, the analytically obtained probability density function of $-\beta\boldsymbol{n}$ in the case of $\boldsymbol{u}=(1,0)$ is shown in Fig. 4. The average of the vectors gives the flow direction.

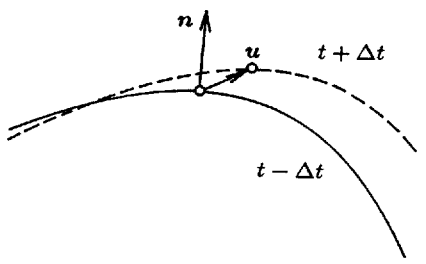

Fig. 3. Displacement of a particle image and its normal vector.

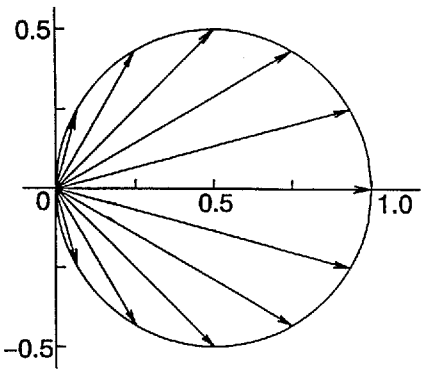

Fig. 4. Diagram for determination of flow direction.

When the sheet illumination is used in the present study, all components of the spatio derivatives ∇f cannot be derived at the same time. Double sheet illumination system is considered to realize the three-dimensional flow field measurement. Figure 5 shows the schematic view of the measurement. Sheet illuminations are given at $x = x_0 + \Delta x$, $x_0 - \Delta x$, and normal to x-axis. Two illuminations are flushed alternately, and the flushing frequency is synchronized to the image capturing. Four images are used for the analysis. The Taylor s expansion can be applied to the luminance function when its change is smooth enough.

$$\begin{aligned} f_i &= f(x_0 - \Delta x, y, z, t_0 - 3\Delta t) \\ &= f(x_0, y, z, t_0) - \frac{\partial f}{\partial x}\Delta x - 3\frac{\partial f}{\partial t}\Delta t + 0(\delta^2), \end{aligned} \tag{14}$$

$$\begin{aligned} f_{i+1} &= f(x_0 + \Delta x, y, z, t_0 - \Delta t) \\ &= f(x_0, y, z, t_0) + \frac{\partial f}{\partial x}\Delta x - \frac{\partial f}{\partial t}\Delta t + 0(\delta^2), \end{aligned} \tag{15}$$

$$\begin{aligned} f_{i+2} &= f(x_0 - \Delta x, y, z, t_0 + \Delta t) \\ &= f(x_0, y, z, t_0) - \frac{\partial f}{\partial x}\Delta x + \frac{\partial f}{\partial t}\Delta t + 0(\delta^2), \end{aligned} \tag{16}$$

$$\begin{aligned} f_{i+3} &= f(x_0 + \Delta x, y, z, t_0 + 3\Delta t) \\ &= f(x_0, y, z, t_0) + \frac{\partial f}{\partial x}\Delta x + 3\frac{\partial f}{\partial t}\Delta t + 0(\delta^2). \end{aligned} \tag{17}$$

Then the derivatives $\partial f/\partial t$, $\partial f/\partial x$ can be obtained as follows.

$$8\frac{\partial f}{\partial t}\Delta t = (f_{i+2} + f_{i+3}) - (f_i + f_{i+1}) \tag{18}$$

$$8\frac{\partial f}{\partial x}\Delta x = (3f_{i+1} + f_{i+3}) - (f_i + 3f_{i+2}) \tag{19}$$

Here $\partial f/\partial y$ and $\partial f/\partial z$ can be obtained by calculating the derivatives on images in each moment, and averaging operation. Then spatio and temporal derivatives are obtained from the four images, and the velocity vectors are calculated in the same process of two-dimensional case.

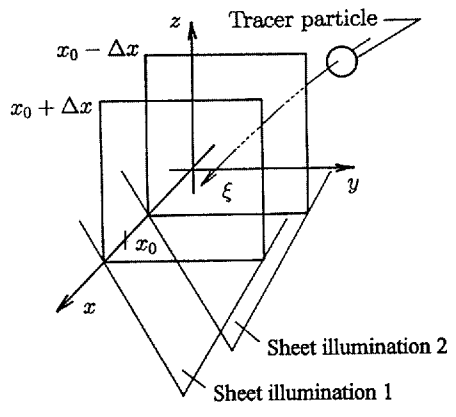

Fig. 5. Schematic view of the measurement in three-dimensional flow field.

4. Least Square Method

The better understanding on the present statistical approach would be achieved by introducing the least square method. The governing equation for the change of visualized flow image is given as shown in Eq.(10). Summation of the quadratic norm can be expressed as,

$$R=\sum_{i=1}^{N}\left(\frac{\partial f_i}{\partial t}+\overline{u}\frac{\partial f_i}{\partial x}+\overline{v}\frac{\partial f_i}{\partial y}+\overline{w}\frac{\partial f_i}{\partial z}\right)^2, \tag{20}$$

where f_i shows the luminance function at $t = t_i$, and $\overline{\boldsymbol{u}} = (\overline{u}, \overline{v}, \overline{w})$ the time-mean velocity at $[t_1, t_N]$. The velocity $\overline{\boldsymbol{u}}$ is given at the minimum point of norm R, and the condition is given as Eq.(21).

$$\frac{\partial R}{\partial \overline{u}}=\frac{\partial R}{\partial \overline{v}}=\frac{\partial R}{\partial \overline{w}}=0. \tag{21}$$

Then $\overline{\boldsymbol{u}}$ is given as the solution of following simultaneous algebraic equations.

$$A\begin{pmatrix}\overline{u}\\ \overline{v}\\ \overline{w}\end{pmatrix}=\begin{pmatrix}-\sum_{i=1}^{N}\left(\frac{\partial f_i}{\partial x}\frac{\partial f_i}{\partial t}\right)\\ -\sum_{i=1}^{N}\left(\frac{\partial f_i}{\partial y}\frac{\partial f_i}{\partial t}\right)\\ -\sum_{i=1}^{N}\left(\frac{\partial f_i}{\partial z}\frac{\partial f_i}{\partial t}\right)\end{pmatrix} \tag{22}$$

$$A=\begin{pmatrix}\sum_{i=1}^{N}\left(\frac{\partial f_i}{\partial x}\right)^2 & \sum_{i=1}^{N}\left(\frac{\partial f_i}{\partial x}\frac{\partial f_i}{\partial y}\right) & \sum_{i=1}^{N}\left(\frac{\partial f_i}{\partial x}\frac{\partial f_i}{\partial z}\right)\\ \sum_{i=1}^{N}\left(\frac{\partial f_i}{\partial y}\frac{\partial f_i}{\partial x}\right) & \sum_{i=1}^{N}\left(\frac{\partial f_i}{\partial y}\right)^2 & \sum_{i=1}^{N}\left(\frac{\partial f_i}{\partial y}\frac{\partial f_i}{\partial z}\right)\\ \sum_{i=1}^{N}\left(\frac{\partial f_i}{\partial z}\frac{\partial f_i}{\partial x}\right) & \sum_{i=1}^{N}\left(\frac{\partial f_i}{\partial z}\frac{\partial f_i}{\partial y}\right) & \sum_{i=1}^{N}\left(\frac{\partial f_i}{\partial z}\right)^2\end{pmatrix} \tag{23}$$

The right hand side of Eq.(22) shows the same contributions with $-\beta\boldsymbol{n}$ as described in the previous section. The diagonal members in the matrix are usually larger than others, and the matrix approaches to the diagonal matrix when the number of sampling is large enough as shown in Eq.(24).

$$\lim_{N\to\infty}\frac{1}{N}\sum_{i=1}^{N}\frac{\partial f_i}{\partial x}\frac{\partial f_i}{\partial y}=\lim_{N\to\infty}\frac{1}{N}\sum_{i=1}^{N}\frac{\partial f_i}{\partial y}\frac{\partial f_i}{\partial z}=\lim_{N\to\infty}\frac{1}{N}\sum_{i=1}^{N}\frac{\partial f_i}{\partial z}\frac{\partial f_i}{\partial x}=0 \tag{24}$$

The final results of the statistical analysis described in the previous sections are equal to the solution of Eq.(22) when matrix A is diagonal. Non-diagonal members in the matrix of A should be considered when the sampling number is small. The contributions of non-diagonal members would appear in the uncertainty of the obtained results as shown in the following numerical simulations.

5. Measurements

The analysis of visualized flow images is examined through experiments and numerical simulations. The measured and calculated results of the flow speed and velocity vector are described in the following sections.

5.1 Flow Speed Measurement

The present method on the flow speed measurement is applied on the measurement of rotating disk. Figure 6 shows the particle-patterned disk which is rotated around the center. The image data were collected by random, and the rotating speed is analyzed. Figure 7 shows the measured rotating speed against the radius r. The relationship of these values can be regarded as linear, and the variance of the measured data increases as r increases. The variance, error band of the random error S, is proportional to the measured flow speed. Figure 8 shows the relative values of random error are uniform in the measurement range.

Wake distribution behind a circular cylinder was measured. A cylinder was installed vertically in a small circulating water channel, and a sheet illumination was given from the bottom of a observation section. The tracer, 500 μm nylon particles, are seeded for visualization. Figure 9 shows the schematic view of the measurement area

and the wake pattern when the Reynolds number $R_n = UD/\nu = 1600$. The dark area represents the low speed area and the bright the high speed. The measured wake pattern shows the shear layer around the edge of the circular cylinder. The convergence is not sufficient so as to find large variance in the result for the 800 pair of images used in this study. High concentration of tracer particles is required for the quick convergence.

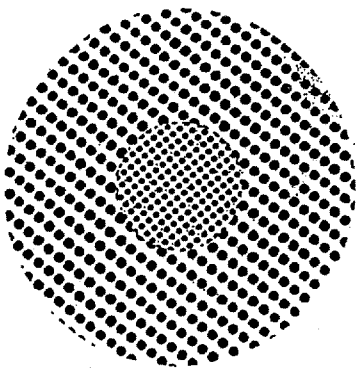

Fig. 6. Particle patterned rotating disk.

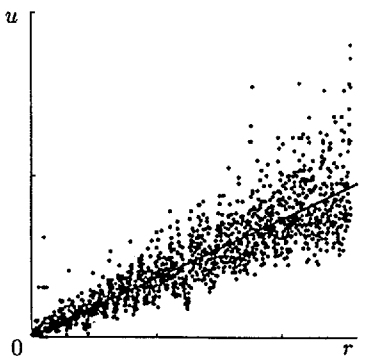

Fig. 7. Measured speed of rotating disk.

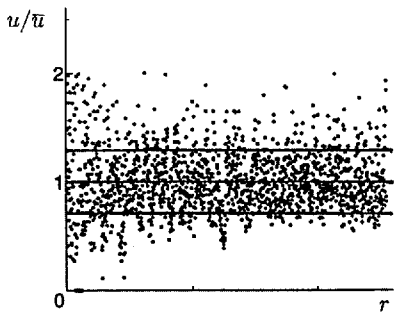

Fig. 8. Measured relative value and random error band.

5.2 Numerical Simulation for Velocity Field

The principle of the velocity field measurement, as shown in Eq.(13), is examined through numerical simulations. The particle images are created numerically. The particle positions are generated using a random function, and the diameter of the particle image is $d = 4.0$(pixel). The particle concentration is 1.25×10^{-2} (1/pixel^2), and the flow velocity is $|\boldsymbol{u}| = 1.0$. The binarized images are used for the analysis, and the spatio derivatives are evaluated by surrounding four pixel data through finite difference scheme. Therefore, the normal vectors of particle images are appeared in eight directions, and the statistical values four directions due to its symmetry. Figure 10 shows the calculated probability distributions of the simulation and the averaged flow vectors. Each vectors represents the possibility of particle passing in its direction. θ represents the given flow direction where $|\boldsymbol{u}| = (\cos\theta, \sin\theta)$, and $\overline{\theta}$

the estimated. The agreements are good at $\theta = 0$, $\pi/4$ due to the symmetry of the distribution. Figure 11 shows the estimated flow direction against the correct angles. $\overline{\theta}$ are smaller at $\theta = [0, \pi/4]$, and larger at $\theta = [\pi/4, \pi/2]$. The digitizing of the images on cell matrix would be the main error factor, i.e., the sensitivities of the derivatives are different in orthgonal direction and horizontal and vertical directions.

5.3 Measurements of Velocity Vectors

The statistical approach is applied on the measurement of velocity vectors. The tracer, 50 μm nylon particles, are used for the visualization here, and the uniform flow with $|\boldsymbol{u}| = 0.02$ m/s is visualized with a sheet illumination given from the bottom. The CCD camera is rotated around its axis for the evaluation of the measurement. Figure 12 shows the velocity distribution obtained from 300 pair of images. It is possible to obtain the velocity vectors at every pixel unit with the present method. Because a high concentration of vectors is achieved, only the center part of the image, 20 $\times$ 20 pixel, is shown in Fig. 12. The convergence is not sufficient, and the absent vectors show the points where the particle passing cannot be observed. Figure 13 shows the mean value of velocity angles in the area. The white marks show the measured values obtained form 100 pair of images, and the black for 300 pair. The solid line shows the exact values, and the measured value is linear against the given angles. Figure 14 shows the comparison of the measurements and the numerical simulations at the same number of sampling. The variance of the measured values is larger than that of the simulation. Larger number of image data or wider area for the averaging is required to achieve higher accuracy.

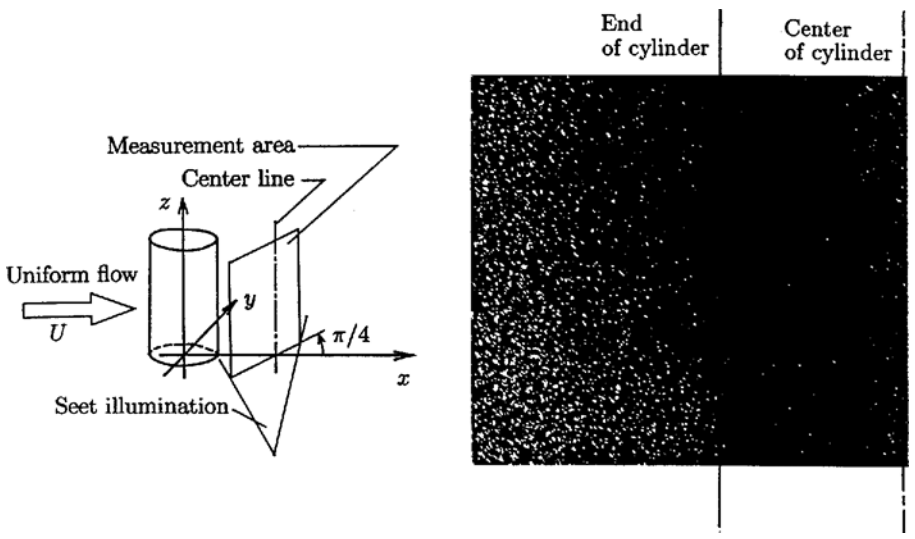

Fig. 9. Schematic view of flow field measurement and measured wake distribution.

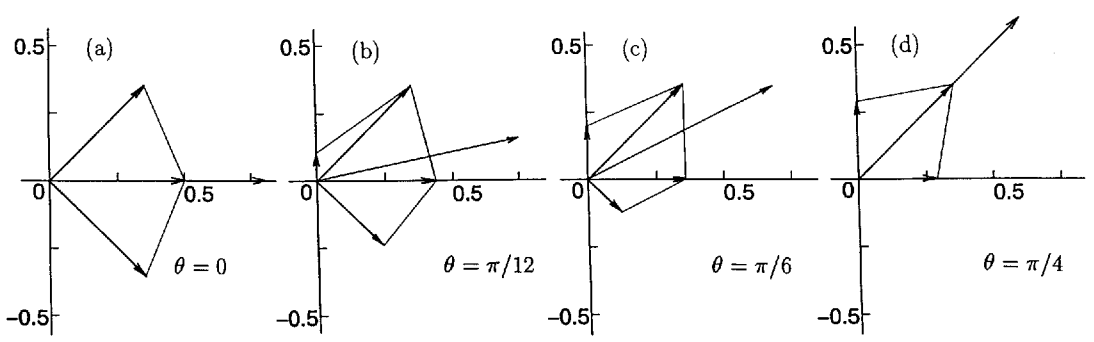

Fig. 10. Calculated probability distribution and flow vector.

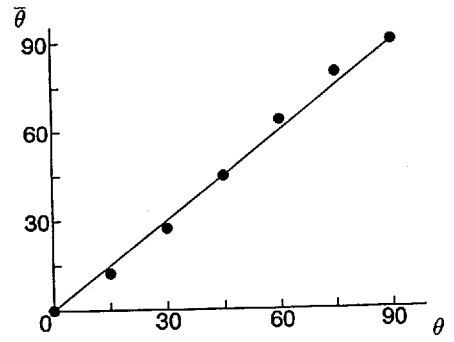

Fig. 11. Comparison of exact velocity direction and the calculated result.

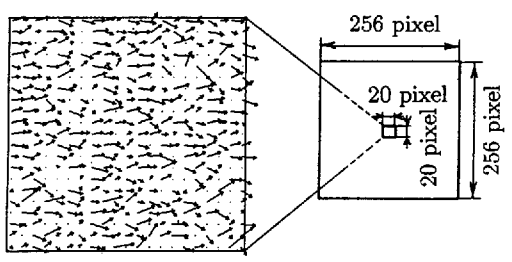

Fig. 12. Measured velocity field through statistical analysis.

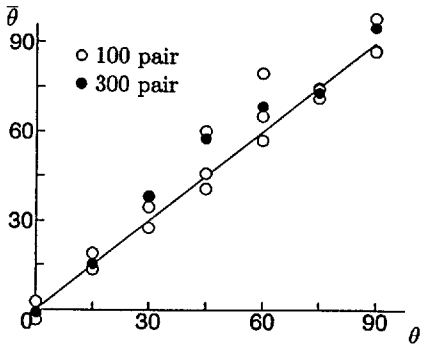

Fig. 13. Measured velocity direction.

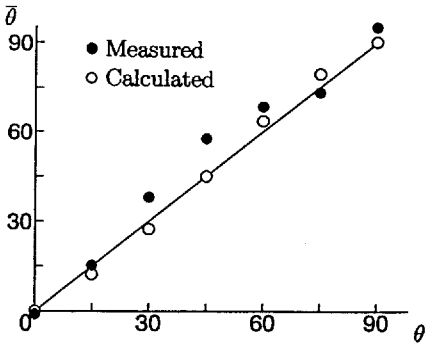

Fig.14. Comparison of the measured and calculated velocity vector.

6. Conclusions

Present paper describes the statistical approach to the measurement of velocity field. The governing equation is formed using the Lagrange s differentiation as same as the gradient method and its vector notation shows that the statistical values of luminance derivatives contain the flow information of velocity vectors. The measurement technique has the pixel unit spatio resolution. The experiments and numerical simulations using the present method are carried out for the two- and three-dimensional flow fields. The three-dimensional flow field measurement is realized by the double sheet illumination system.

The dynamic range of present technique is limited, and the short time interval between the images is required to increase the range. The measurement technique would be useful in the wide practical flows because of the simple analysis process and system even in the case of three-dimensional flow.

Acknowledgements

The authors would like to express their appreciation to Mr. Kimoto, Kawasaki Heavy Industry, and Mr. Kawashita, under graduate student of Osaka Prefecture University, for their experimental works, and Miss Hirata, graduate student of OPU, for her support on the numerical simulations.

References

Ando, S., A Vector Field Measurement System Based on Spatio-Temporal Image Derivative, Trans. of Soc. of Instru. and Control Eng., 22-12 (1986), 1330-1336.

Fukinuke, Y., Digital Signal Analysis of Images, (1981), Daily News on Ind. Co. Ltd.

Hildreth, E. C., Computation Underlying the Measurement of Visual Motion, Artificial Intelligence, 23 (1984), 309-354.

Horn, B. K. P. and Schunk, B. G., Determining Optical Flow, Artificial Intelligence, 17 (1981), 185-203.

Kobayashi, M., An Application of Spatial Filtering, Jour. of the Soc. Instr. Control Eng., 19-6 (1980), 571-579.

Katoh, Y., Miyamoto, M., Kaneko, S., Miike, H. and Koga, K., Image Analysis with Spatial Filtering Method for Fluidizing Particle Velocity in a Circular Fluidized Bed, Proc. of the 6th Inter. Symposium on Flow Visualization, (1992), 740-744.

Nishio, S., Okuno, T. and Kimoto, N., Development of Image Measurement System by Means of Statistical Analysis, Jour. of Kansai Soc. of Naval Architecture, Japan, 224, (1995), 27-34.

Nishio, S. and Okuno, T., Development of Image Measurement System by Means of Statistical Analysis (2nd Report: General Form of Governing Equation), Jour. of the Kansai Soc. of Naval Architecture, Japan, 225 (1996), 67-74.

Okuno, T. and Nakaoka, J., Velocity Field Measurement by Spatio-Temporal Derivative Method, Jour. of the Kansai Soc. of Naval Architecture, Japan, 215 (1991), 69-74.

Okuno T., Nishio, S. and Yoshino, Y., Flow Field Measurement Method by Means of Time-Averaged Contrast of Image, Jour. of Kansai Soc. of Naval Architecture, Japan, 219 (1993), 19-23.

Okuno, T., Nishio, S. and Kimoto, N., Time Mean Velocity Field using Visualized Flow Image, Jour. of Flow Visualization and Image Processing, 1 (1994), 385-392.

Authors' Profiles

Shigeru Nishio: He has graduated from Osaka University in 1983 and has received his M. Eng. degree in Naval Architecture in 1985. He has been working in Department of Naval Architecture, Osaka Prefecture University since 1988, and was awarded Dr. Eng. degree in ship hydrodynamics, study on the three-dimensional separated flow around prolate spheroids and ships at incidence in 1990. He works as an associate professor in Osaka Prefecture University, Department of Marine System Engineering since 1996. His research interests are in the image measurement of flow field, and bio-fluid mechanics in fish-like propulsions.

Taketoshi Okuno: He has graduated from Osaka Prefecture University in 1969 and has received his M. Eng. degree in Naval Architecture in 1971. He has been working in Department of Naval Architecture, Osaka Prefecture University since he had completed the master degree course in graduate school of engineering. He has obtained his Dr.Eng. degree in the field of Naval Architecture, three dimensional boundary layer around ship hull in 1980. He worked for the University of Liverpool from 1982 to 1984 as a research fellow. He works as a professor in Osaka Prefecture University, Department of Marine System Engineering since 1991. His research interests are in image measurement of flow field, and also various measurements in coastal zone.